



# Genome-wide identification and analysis of the *SGR* gene family in *Cucumis melo* L.

R.G. Bade<sup>1,2</sup>, M.L. Bao<sup>1</sup>, W.Y. Jin<sup>1</sup>, Y. Ma<sup>3</sup>, Y.D. Niu<sup>1</sup> and A. Hasi<sup>1</sup>

<sup>1</sup>Inner Mongolia Key Laboratory of Herbage & Endemic Crop Biotechnology, School of Life Sciences, Inner Mongolia University, Hohhot, China

<sup>2</sup>Biomedical Research Center of Center Laboratory, Baotou Medical College, Baotou, China

<sup>3</sup>Department of Biological Science and Technology, Baotou Teacher's College, Baotou, China

Corresponding author: A. Hasi

E-mail: hasind@sina.com

Genet. Mol. Res. 15 (4): gmr15048485

Received January 25, 2016

Accepted August 22, 2016

Published October 17, 2016

DOI <http://dx.doi.org/10.4238/gmr15048485>

Copyright © 2016 The Authors. This is an open-access article distributed under the terms of the Creative Commons Attribution ShareAlike (CC BY-SA) 4.0 License.

**ABSTRACT.** Chlorophyll (CHL) is present in many plant organs, and its metabolism is strongly regulated throughout plant development. Understanding the fate of CHL in senescent leaves or during fruit ripening is a complex process. The stay-green (SGR) protein has been shown to affect CHL degradation. In this study, we used the conserved sequences of STAY-GREEN domain protein (NP\_567673) in *Arabidopsis thaliana* as a probe to search SGR family genes in the genome-wide melon protein database. Four candidate *SGR* family genes were identified in melon (*Cucumis melo* L. Hetao). The phylogenetic evolution, gene structure, and conserved motifs were subsequently analyzed. In order to verify the function of *CmSGR* genes in CHL degradation, *CmSGR1* and *CmSGR2* were transiently overexpressed and silenced using different plasmids in melon. Overexpression of *CmSGR1*

or *CmSGR2* induced leaf yellowing or fruit ripening, while silencing of *CmSGR1* or *CmSGR2* via RNA interference delayed CHL breakdown during fruit ripening or leaf senescence compared with the wild type. Next, the expression profile was analyzed, and we found that *CmSGR* genes were expressed ubiquitously. Moreover, *CmSGR1* and *CmSGR2* were upregulated, and promoted fruit ripening. *CmSGR3* and *CmSGR4* were more highly expressed in leaves, cotyledon, and stem compared with *CmSGR1* or *CmSGR2*. Thus, we conclude that *CmSGR* genes are crucial for fruit ripening and leaf senescence. *CmSGR* protein structure and function were further clarified to provide a theoretical foundation and valuable information for improved performance of melon.

**Key words:** Melon; Stay-green; Bioinformatic analysis; Chlorophyll degradation; Leaf senescence

## INTRODUCTION

As a photoreceptor, chlorophyll (CHL) is a key component of the photosynthesis machinery and is required for the absorption of sunlight. CHL exists in chloroplast membranes where it is bound in CHL-protein complexes (Markwell et al., 1979). The protein components of the two photosystems are structurally organized into morphologically distinct membrane subunits (Arntzen, 1978), including photosystem I (PSI) and photosystem II (PSII) reaction center complexes (Kusaba et al., 2007). The final step of leaf and fruit development is senescence and degradation, which is an active process that salvages nutrients from the fruit and leaf (Matile, 2000; Pruzinská et al., 2005; Hörtensteiner and Kräutler, 2011). Leaf senescence is a complex process in which multiple cellular events proceed in parallel or sequentially. Furthermore, this process requires a lot of energy, and involves a sequence of physiological and biochemical events (Lim et al., 2007; Procházková and Wilhelmová, 2007). These events are characteristically followed by the breakdown of nuclei, plastids, vacuoles, and mitochondria, and ultimately lead to cell death (Buchanan-Wollaston, 1997).

Mutants that retain green pigments during senescence are collectively called stay-green (or non-yellowing) mutants, and have been isolated from several plants (Grassl et al., 2012). Stay-green or non-yellowing mutants have been of high interest in the determination of genetic and biochemical mechanisms of CHL breakdown during leaf senescence and fruit ripening. Earlier stay-green mutants have been reported to maintain greenness in leaf or fruit longer than in wild-type plants during senescence (Thomas and Smart, 1993; Spano et al., 2003; Hörtensteiner, 2009). The breakdown of CHL is catalyzed by several CHL catabolic enzymes in an enzymatic process (Rong et al., 2013). Several genes (*SGR*, *RCCR*, *PAO*, *PPH*, *NYCI*, and *NOL*) regulating the process of leaf senescence and fruit ripening have been identified (Lim et al., 2003; Hörtensteiner and Kräutler, 2011; Luo et al., 2013). Senescence-associated gene (*SGR*) plays a critical role in the regulation of CHL degradation and senescence. In addition, *SGR* is typically upregulated during senescence (Ren et al., 2007; Hörtensteiner, 2009). Chloroplast-located proteins encoded by *SGR* genes in different species are well conserved in higher plants, and it is expected that *SGR* interacts with subunits of the light harvesting complex of PSII (Park et al., 2007; Hörtensteiner, 2009). In recent years, the functions of the products of *SGR* genes have been identified in *Arabidopsis thaliana* (Sakuraba

et al., 2012), *Oryza sativa* (Jiang et al., 2007), *Pisum sativum* (Sato et al., 2007), *Solanum lycopersicum* (Akhtar et al., 1999; Luo et al., 2013), *Triticum aestivum* (Spano et al., 2003), and other species. Expression of *SGR* in *Arabidopsis* and tobacco induces the degradation and senescence of leaf CHL (Park et al., 2007; Ren et al., 2007; Grassl et al., 2012). Silencing of *SGR* by RNA interference (RNAi) leads to reduced CHL degradation in leaves and fruits (Hu et al., 2011; Zhou et al., 2011; Luo et al., 2013).

In this study, we performed a predictive computer analysis for *SGR* genes in melons, and four putative *SGR* genes were identified from the MELONOMICS (<https://melonomics.net>) database, which includes CM\_protein\_v3.5, melon\_genome pseudomolecules v3.5. Phylogenetic analyses were performed and gene structures were compared to reveal the evolutionary relationships among *SGRs*. The transient expression of *SGR* by agro-infiltration in melon fruit may enhance chlorophyll degradation, while silencing of *SGR* by RNAi with agro-infiltration in melon fruit resulted in reduced chlorophyll degradation. In addition, to demonstrate the spatial patterns of *SGR* family gene expression, gene expression in seven tissues was analyzed.

## MATERIAL AND METHODS

### Identification of the *SGR* family in melon

To identify members of the *SGR* gene family in melon, multiple database searches were performed. An *A. thaliana* protein with a typical STAY-GREEN domain structure was selected as the query sequence in the National Center for Biotechnology Information (NCBI) database (accession No. NP\_567673), using BLASTp (Altschul et al., 1990) at E values  $\leq 10^{-3}$  to avoid false positives, and *SGR* family genes were searched in the melon genome. CM\_protein\_v3.5 (<https://melonomics.net/files/Genome>), which was used as a search database for local BLASTp. BioEdit 7.0.9 (Hall, 1999) was used to analyze homologs of *SGR* family genes in local BLASTp. We also performed database searches using amino acid sequences of the STAY-GREEN domain of other members of the *A. thaliana* *SGR* family as the query to confirm the completeness of the collection. To confirm the putative *SGR* family genes, amino acid sequences were searched for the STAY-GREEN domain using the Simple Modular Architecture Research Tool (SMART) (Schultz et al., 1998; Letunic et al., 2004). The Pfam (<http://pfam.sanger.ac.uk/search>) and SMART (<http://smart.embl-heidelberg.de/>) databases were used to confirm each predicted melon *SGR* protein sequence.

### Gene structure analysis of the melon *SGR* genes

Information on melon *SGR* genes, including accession number, open-reading frame (ORF) length, and exon-intron structure, was retrieved from CM\_protein\_v3.5 (<https://melonomics.net/files/Genome>).

### Phylogenetic analysis and characterization of melon *SGR* proteins

Multiple alignments of *SGR* proteins were carried out using the Clustal W (<http://bioinformatics.ubc.ca/resources/tools/clustalw>) program (Chenna et al., 2003). DNAMAN software (Version 7.0) was also used as a secondary tool to align sequences and calibrate

the results. Phylogenetic trees were constructed using MEGA 6.0 software (<http://www.megasoftware.net/mega.html>) (Tamura et al., 2013) with the neighbor-joining (NJ) method (Saitou and Nei, 1987) and the 1000-bootstrap replicates. The phylogenetic trees were drawn with MEGA 6.0, and the Multiple Em for Motif Elicitation (MEME) program v4.9.0 (<http://meme-suite.org/tools/meme>) (Bailey et al., 2009) was used to predict potential motifs in the putative SGR family gene sequences with the following parameters: optimum width of 6-50 amino acids, and the maximum number of motifs was set to five. The significance of the resulting motifs was checked in the NCBI and SMART databases (Sharma et al., 2010).

### Plant materials and growth conditions

Melon (*Cucumis melo* L. cv Hetao) plants were used for the experiments and were grown in the field. Self-pollination was performed by hand and the pollination time was recorded and controlled between 9:00 and 11:30 a.m. Each plant retained only one fruit. The injected tissues were sampled and harvested with phenotypes. The mesocarp was frozen in liquid nitrogen after collection and then stored at -80°C for subsequent extraction of total RNA.

### Vector construction and *Agrobacterium*-based transient transformation

Total RNA was isolated from melon fruit mesocarp. The full-length cDNA of *CmSGR1* and *CmSGR2* was amplified, using the forward primer: 5'-TTAATTTTATAGATGGCGAGAT-3' and 5'-TCTGTTGGAGAAGATGAGGGTT-3', and the reverse primer: 5'-GGGAGCCAAATAAAATCAAT-3' and 5'-TAAGGGGGAGCCAAATAAAATC-3', respectively. Amplified fragments of these genes were cloned into the *pEASY*<sup>®</sup>- Blunt Cloning Vector (TransGen, China), according to the manufacturer instructions, and sequenced. These were then cloned into the pZP221 (35S-NOS) and pART27, using the primers detailed in [Table S1](#). All vectors were transferred into *Agrobacterium tumefaciens* AGL1 by the freeze-thaw method, and subsequently the *Agrobacterium* were used for agroinfiltration into melon fruit.

*Agrobacterium* cultures (5 mL) were grown overnight from single colonies in *Agrobacterium rhizogenes* culture (YEB) medium plus selective antibiotics (rifampicin 50 mg/L, spectinomycin 20 mg/L), at 28°C, 175 rpm, which were then transferred into 50-mL induction medium (0.5% peptone, 0.5% beef extract, 0.1% yeast extract, 0.5% sucrose, 2 mM MgSO<sub>4</sub>, 20 μM acetosyringone, 10 mM MES, pH 5.6) plus antibiotics (rifampicin 50 mg/L, spectinomycin 20 mg/L), and grown overnight to the log phase (OD ≈ 0.8), at 28°C, 180 rpm. *Agrobacterium* cultures were recovered by centrifugation and resuspended in MMA medium (10 mM MgCl<sub>2</sub>, 10 mM MES, 200 μM acetosyringone, pH 5.6) plus 100 mg/L 2, 4-dichlorophenoxyacetic acid and 0.005% Tween-20. The *Agrobacterium* suspension was incubated at room temperature with gentle agitation (20 rpm) for a minimum of 2 h and then used for infiltration medium and injected in the fruits. Agroinjection was performed as follows: melon fruits at different stages of development were infiltrated using a 1-mL syringe with a 0.7 x 30-mm needle, which was introduced 5 to 7 mm in depth. The infiltration medium was slowly injected into the fruit. The total volume of solution injected varied at different developmental stages, with a maximum volume of 1000 μL injected into mature green melons.

## RNA isolation and real-time quantitative RT-PCR expression analysis

Total RNA was extracted using RNAiso plus for polysaccharide-rich plant tissue (TaKaRa, Japan) according to the manufacturer instructions. Total RNA extracts were analyzed by UV spectrophotometry and agarose gel electrophoresis. Contaminated DNA was removed with RNase-free DNase I (TaKaRa) treatment. First-strand cDNA was reverse transcribed from 0.5 µg total RNA from melon fruits at various stages of development and ripening and other tissues, and was used as a template in a 10-µL reaction mixture using PrimeScript™ RT Master Mix (Perfect Real Time) (TaKaRa) according to the manufacturer instructions. The primer sequences are listed in [Table S2](#). Amplification of melon glyceraldehyde 3-phosphate dehydrogenase (GAPDH) gene was used as an internal control to calculate the relative fold differences based on the comparative Ct method. cDNA was amplified with SYBR® Premix Ex Taq™ (Perfect Real Time) (TaKaRa) using the Opticon 3 real-time system (BioRad, USA) in a 25-µL volume. Melting curves were generated immediately after the last cycle to exclude any influence of primer dimers. Cycle numbers, representing the point at which the fluorescence passed the cycle threshold (Ct), were analyzed, and the relative expression was calculated by the  $2^{-\Delta\Delta C_t}$  method. At least three technical and three biological replicates were performed for each reaction. Data points in the quantitative real-time PCR (qRT-PCR) time course are reported as means ± SE of three biological replicates.

## RESULTS

### Genome-wide identification of the SGR family in melon

To detect candidate SGR homologs in the melon genome, the SGR domain of a melon SGR amino acid sequence was used as a protein BLAST query sequence using the MELONOMICS database. Four candidate SGR sequences were identified as potentially containing the SGR domain (Table 1). In order to verify its reliability, the *A. thaliana* SGR family was used as the query (accession No. NP\_567673), and the results were consistent with the initial search. Four equivalent sequences were obtained using the MELONOMICS database by hidden Markov model analysis with PF12638, which contains a typical SGR domain (Table 1). SMART analysis indicated that the SGR domain of each of the four *CmSGR* sequence was typical in order to verify their reliability. Using those methods, five SGRs from *A. thaliana* (B3H593, Q66WT5, 891373, Q94AQ9, and O82741) and three SGRs from *S. lycopersicum* (NP\_001234723, XP\_004252642, and XP\_004237702), two SGRs from the *Cucumis sativus* genome (Cucsa.302630 and Cucsa.077260) were detected ([Table S3](#)).

**Table 1.** Analysis of amino acid composition and physical/chemical properties of the *CmSGR* genes.

Gene name	Sequence ID	chr	Start	Stop	ORF length (bp)	Exon number	Intron number	Length (aa)	MW (kDa)	pI
<i>CmSGR1</i>	MELO3C005616T1	9	6492669	6494594	651	3	2	216	24.8365	7.07
<i>CmSGR2</i>	MELO3C005616T2	9	6492669	6495151	774	4	3	257	29.4819	8.72
<i>CmSGR3</i>	MELO3C008435T1	3	6153941	6155462	597	4	3	198	22.4940	8.69
<i>CmSGR4</i>	MELO3C008435T2	3	6154472	6155462	504	3	2	167	19.0230	6.19

*CmSGR*: *Cucumis melo* stay green protein; ORF: open reading frame; MW: molecular weight; pI: isoelectric point.

## Structure analysis of the melon *SGR* genes

*CmSGR* ORF lengths ranged from 504 (*CmSGR4*) to 774 bp (*CmSGR2*), molecular weights ranged from 19.02 (*CmSGR4*) to 29.48 kDa (*CmSGR2*), and pI values ranged from 6.19 (*CmSGR4*) to 8.72 (*CmSGR2*) (Table 1). *CmSGR* genes were distributed on all chromosome of the melon genome. *CmSGR1* and *CmSGR2* genes were located on chromosome 9, and the another two were detected on chromosome 3. Based on the exon and intron structures, the number of introns differed. The number of introns in the *CmSGR2* or *CmSGR3* genes was three, while *CmSGR1* and *CmSGR4* genes contained two (Table 1 and Figure 1). Although, the protein analysis programs SMART and Pfam (Finn et al., 2014) could be used to analyze the major domains encoded by the *CmSGR1*, those programs were unable to identify smaller individual motifs. Hence, we used the MEME database to recognize further motifs and conserved domains shared within the SGR gene family. The motifs identified by MEME were between 6 and 50 amino acids in length. Five common motifs were observed, but the biological functions of these motifs were not known. Structure analysis revealed that the STAY-GREEN domain at the N-terminal was highly conservative. A chloroplast transit peptide was conserved motif near the N-terminal. The domains I, II, and III formed the STAY-GREEN domain. The C-terminal containing domain III possessed 2 to 6 conserved glutamines (Q) (Figure 2). Motifs 1, 2, 3, and 5 formed the configurations of the SGR domain I. Motif 4 was distinctively detected in *CmSGR1* and *CmSGR2*, and formed domain II. Motif 4 determined C-X3-C-X-C2-F-P-X5-P domain in C-terminal conservative amino acid sequence, which was the highly homologous core region of SGRs, but the Motif 4 was deleted in *CmSGR3* and *CmSGR4*. (Table 2 and Figure 3).

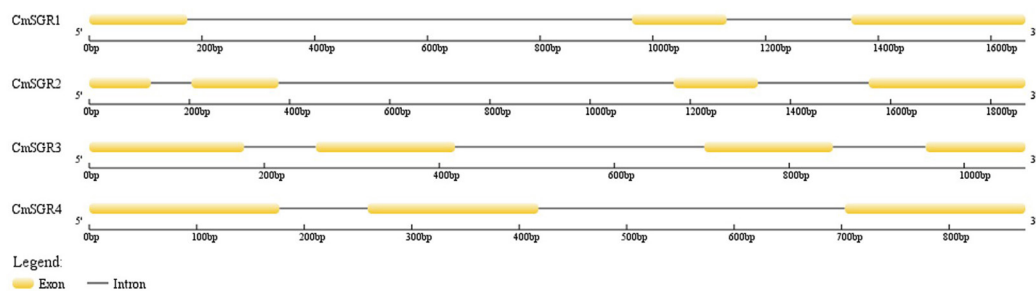


**Figure 1.** Structure of the *CmSGR* genes. Exons and introns are depicted by filled yellow boxes and single lines, respectively.

## Phylogenetic and structural analyses

To explore the classifications and phylogenetic relationships of SGR proteins, we carried out phylogenetic analyses on different SGR proteins from different sequenced genomes of plants. Comprising *A. thaliana*, *S. lycopersicum*, and *C. sativus*, information on the SGR family was listed in [Table S3](#). Full-length protein sequences from plants were used to construct an unrooted NJ phylogenetic tree, which was generated from the aligned full-length protein sequences of all four *CmSGRs*, five *AtSGRs*, three *SISGRs*, and two *CsSGRs*. *Arabidopsis*, cucumber, tomato, and melon SGR proteins were grouped into two subfamilies via analysis of phylogenetic tree with well-supported bootstrap values (1000 replicates). The resulting

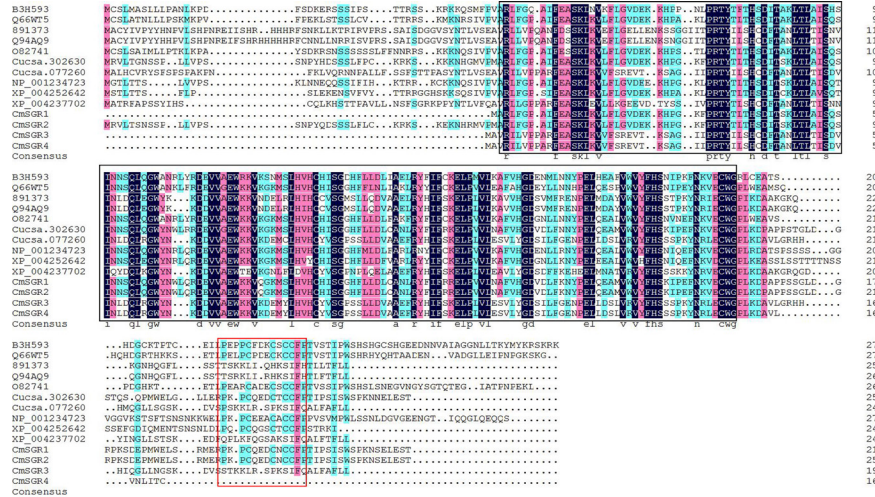


**Figure 2.** Sequence alignment of SGR proteins from melon and other higher plant species. *Arabidopsis* (B3H593, Q66WT5, 891373, Q94AQ9, O82741), tomato (NP\_001234723, XP\_004252642, XP\_004237702), and cucumber (Cucsa.302630, Cucsa.077260) proteins belonging to SGR protein alignments base on the highly conserved central core of the STAY-GREREN domain were performed using DNAMAN Version 7.0. Sequences consisting of the cysteine-rich motif (C-X3-C-X-C2-F-P-X5-P) defined by Aubry et al. (2008) are shown in the red frame, Black shading with white letters, pink shading with white letters, and blue shading with black letters indicate 100, 75, and 50% sequence identity, respectively.

**Table 2.** Analysis of conserved motifs in the CmSGR family in melon.

Motif	Sequence logo
Motif 1	
Motif 2	
Motif 3	
Motif 4	
Motif 5	

phylogenetic tree demonstrated that CmSGRs share and evolutionary close relationship with CsSGRs. CmSGR1 and CmSGR2 were grouped into the first subfamily, and these two melon genes were clustered with CsSGR based on high sequence similarity with Cucsa.302630. The two external nodes at the end of the same clades of the phylogenetic tree were likely to represent the closest homologous gene pairs. The phylogenetic tree showed that CmSGR1 and CmSGR2 in the same clade were duplicated several times before the formation of melon species, and that this occurred after repeated events, which was similar to AtSGRs (Q66WT5

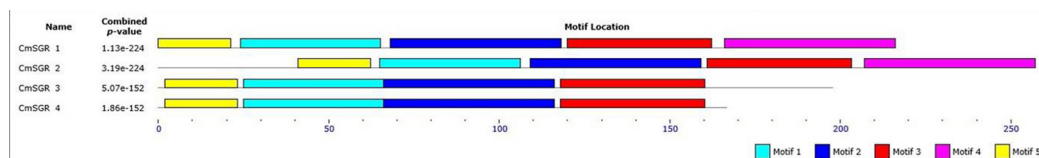


**Figure 3.** Distribution of conserved motifs in four CmSGR proteins. The distribution of five conserved domains, represented by the colored boxes, was identified using CmSGR protein sequences in MEME suite 4.10.1. The order of the motif corresponds to their position in the individual protein sequences.

and O82741, 891373 and Q94AQ9) and SISGRs (NP\_001234723 and XP\_004252642) in *Arabidopsis* and tomato gene families. CmSGR3 and CmSGR4 were grouped in the second subfamily, and were most homologous to CsSGR (Cucsa.077260). Melons and cucumbers belong to the cucurbit family, and SGRs were clustered together and were less evolved following speciation. However, in *Arabidopsis*, those genes were generated through long-term evolution and might have species-specific functions. The combined phylogenetic analysis revealed that the ancestral gene of the SGR family originated from the divergence of other species and repeated events (Figure 4).

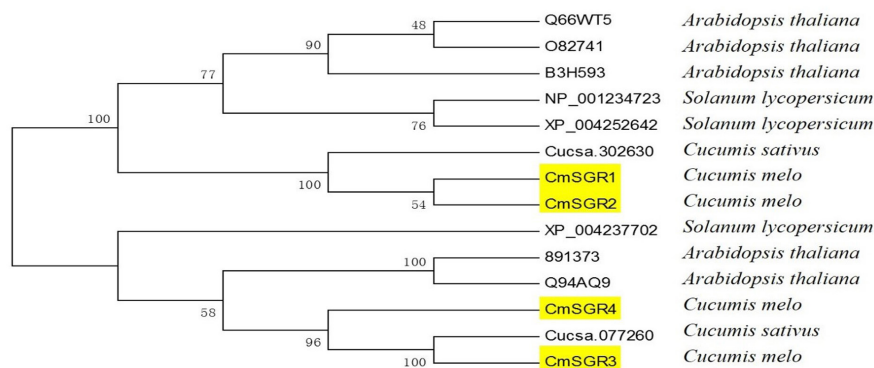


**Figure 4.** Phylogenetic relationships among melon, tomato, cucumber, and *Arabidopsis* SGR proteins. Neighbor-joining tree was created using the MEGA6.0 program (bootstrap value set at 1000) with full-length sequences of four melon SGR proteins (MELO3C005616P1, MELO3C005616P2, MELO3C008435P1, MELO3C008435P2) with yellow shading, three tomato (NP\_001234723, XP\_004252642, XP\_004237702), two cucumber (Cucsa.302630, Cucsa.077260), and five *Arabidopsis* (B3H593, Q66WT5, 891373, Q94AQ9, O82741) proteins.

### Infiltration of melon fruit tissues with *Agrobacterium*

To confirm the function of the *SGR* gene in melon fruits, Oe-CmSGR (overexpressing) (p35S-SGR1, p35S-SGR2) and CmSGR-RNAi (pART27-SGR1, pART27-SGR2) vectors were constructed and introduced into melon fruit by *Agrobacterium*-based transient transformation. *Agrobacterium* cultures containing p35S-SGR1, p35S-SGR2, pART27-SGR1, pART27-SGR2, pPZP221 (35S-NOS), and pART27 were syringe-infiltrated into the mesocarp (mature green), respectively. About 5-7 days after infiltration, approximately 50% of the infiltrated fruit (total 50 pieces) was discarded because of decay and other factors, but the phenotype of the Oe-CmSGR1 (16%), and Oe-CmSGR2-infiltrated fruit (14%) turned a yellow color. However, control fruit infiltrated with pPZP221-35S-NOS and *Agrobacterium* cultures alone remained green, with a similar phenotype to the wild type (WT) fruit (Figure 5A, 5B, 5C). There was



increased expression of *SGR* at the mature green stage, and the highest level was reached at the Breaker stage, where expressed induced by ripening was observed. Compared with non-injection fruit, at about B+7 (7 days after breaker), the pART27-*SGR1* (16%) and, pART27-*SGR2*-infiltrated fruit (12%) exhibited a delay in turning yellow at the injection site (stay green), and a green phenotype was retained for at least 7-10 days (Figure 5D, E, F). Approximately 40% of the infiltrated fruit (total 50 pieces) was discarded. Those results suggested that *CmSGR*-RNAi suppressed *CHL* degradation and exhibited a stay-green phenomenon, whose function was similar to that of the *LeSGR1* gene in tomato plants (Hu et al., 2011).



**Figure 5.** Recombinant vectors were used to infect melon fruit by *Agrobacterium*-based transient transformation. pPZP221-35S-NOS (A) and pART27 (D) plasmids were used as the control. Detached mature green melon fruits were infiltrated with *Agrobacterium* and transformed with p35S-*SGR1* (B) and p35S-*SGR2* (C) (overexpressing), pART27-*SGR1* (E), and pART27-*SGR2* (F) (RNAi). Ov-*CmSGR* was upregulated and promoted fruit ripening, which exhibited a yellow color phenotype, while *CmSGR*-RNAi inhibited chlorophyll degradation and exhibited a stay-green phenotype.

### ***SGR* gene expression in different tissues and at developmental stages**

To determine the involvement of *SGR* genes in growth and development during the melon life cycle, the expression profile of *SGR* family genes under normal growth conditions was investigated by qRT-PCR in various tissues, including the root, stem, leaf, and fruit at 10, 20, 30, 40 (breaker stage), and 45 days after pollination (DAP). The results indicated that *SGRs* were expressed in all tissues (Figure 6). *CmSGR1* and *CmSGR2* were expressed at relatively high levels in cotyledon and at 45 DAP, with fruit maturation. Expression of *CmSGR1* and *CmSGR2* was increased, and the highest expression was observed at 45 DAP. We speculated that *CmSGR1* and *CmSGR2* might be related to fruit development and leaf senescence. However, *CmSGR3* and *CmSGR4* were more highly expressed in leaves and cotyledon than in fruit and root (5-fold increase). As the fruits develop, the expression levels of *CmSGR3* and *CmSGR4* continuously decreased from 10 to 30 DAP, and slightly increased from 30 to 45 DAP. The results indicated that expression of *CmSGR3* and *CmSGR4* were increasing during fruit ripening and *CHL* degradation.

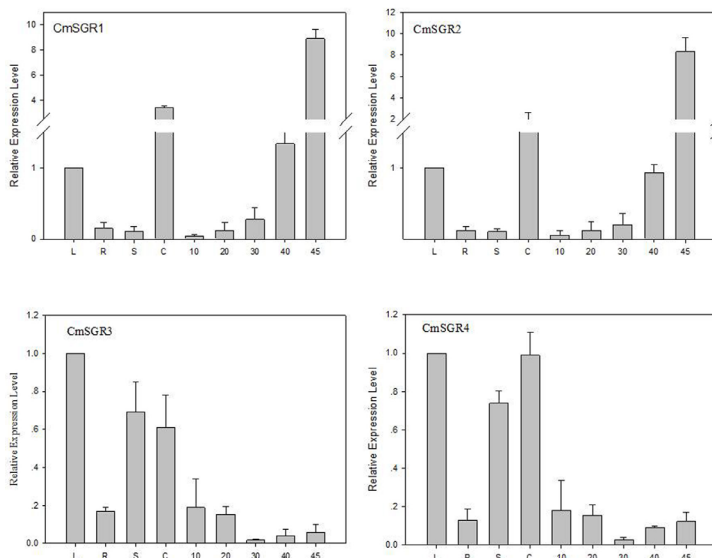


**Figure 6.** Tissue-specific expression profiles of four *CmSGR* genes in different melon organs. The Y-axis represents the relative transcript abundance. The X-axis represents melon tissues. Total RNA was isolated from leaves (L), roots (R), stems (S), cotyledon (C), and fruit (10, 20, 30, 40, and 45 DAP), respectively. Bars represent standard deviations (SD) of three technical replicates, plotted as mean  $\pm$  SE of three biological replicates. GAPDH (accession No. MELO3C002342T1) gene in melon was used as an internal control.

## DISCUSSION

CHL degradation is an important process of senescence and is a characteristic of fleshy fruit, in combination with anthocyanin accumulation and carotenoid retention (Park et al., 2007). CHL degreening is associated with the upregulation of CHL degradation and downregulation of CHL biosynthesis. In several fruits including melon, fruit color is used as an index of maturity. *SGR* genes have been observed in *sgr* mutants and are upregulated during senescence. In many crops, stay-green genotypes have also been shown to enhance resistance to disease and drought and possess leaves. In our study, we used *SGR* gene and protein sequences from *A. thaliana* as probes to identify *CmSGR* genes from *C. melo* L. Hetao, which were used to investigate the molecular mechanism of color development during ripening. Finally, four non-redundant *SGR* genes were identified and characterized in the melon genome. Although the *C. melo* genome is approximately 3-fold larger than the *Arabidopsis* genome (375 and 125 Mb, respectively) (Arabidopsis Genome Initiative, 2000; Garcia-Mas et al., 2012), the gene number in *C. melo* is less than that in *Arabidopsis* (4:7). Those results suggested that gene loss had occurred during genome duplication, the gene number in *C. melo* is 2-fold the *SGR* genes of *C. sativus* (4:2), and it probably support the idea that these *SGR* genes was highly conserved in monocot and dicot plant species.

It is widely accepted that the pattern of intron/exon positions helps in the understanding of evolutionary relationships (Hu and Liu, 2011). In the *SGR* genes from melon, *CmSGR2* and *CmSGR4* contain three introns, *CmSGR3* contains four 4 introns, and *CmSGR1* contains two introns (Table 1). Phylogenetic analysis showed that melon *SGR* proteins clustered more

closely with those from cucumber than with those from *Arabidopsis* and tomato, including highest bootstrap values of 100% in cucumber (Figure 4). There was an apparent parallel relationship between the structure of genes and the phylogeny of branches during in the late stages of evolution. The exon/intron pattern of the *SGR* genes may be stable in melon and cucumber. While lower bootstrap values were found between CmSGR1 and CmSGR2 (54%), higher bootstrap values were found between CmSGR3 and CmSGR4 (96%) (Figure 4) in the joined tree. This may be related to the structures of SGRs and may reflect the functional conservation of plant SGRs. MEME analysis revealed there was extensive conservation in the motif pattern within the SGR; the N-terminal is the putative chloroplast transit peptide region (motif 5). A Cys-rich motif (C-X3-C-X-C2-F-P-X5-P) is present in the C-terminal of the SGR proteins but not in the SGR-like proteins, with a variable region of 12 to 38 amino acids in length (Aubry et al., 2008; Pilkington et al., 2012). However, this motif is absent from the CmSGR3 and CmSGR4 proteins. The four conserved Cys residues, which may account for the activity of the catalytic site, may have functions in intermolecular or intramolecular crosslinking or may be involved in redox regulation (Aubry et al., 2008).

The up- or downregulation of *SGR* gene expression during leaf senescence or fruit ripening coincides with CHL degradation (Jiang et al., 2007; Kusaba et al., 2007; Park et al., 2007; Tang et al., 2011; Luo et al., 2013). To investigate the function of the *CmSGR* genes in CHL degradation, we performed a test to determine whether SGR expression could induce leaf yellowing or fruit ripening. We used the Oe-CmSGR plasmid to overexpression of the *CmSGR* and *CmSGR*-RNAi vector to repress the activity of endogenous *CmSGR* in melon. Oe-*CmSGR* (p35S-*SGR1*, p35S-*SGR2*) and *CmSGR*-RNAi (pART27-*SGR1*, pART27-*SGR2*) vectors were constructed and introduced into melon fruit by *Agrobacterium*-based transient transformation. *Agrobacterium* cultures containing p35S-*SGR* or pART27-*SGR* constructs were syringe-infiltrated into the mesocarp. After 5-7 days infiltration, the fruits were infiltrated with the p35S-NOS vector whether or not the fruits were retained the stay-green phenotype in control group. However, the fruits infiltrated with p35S-*SGR1* or p35S-*SGR2* developed a yellow color. *SGR* gene expression analysis showed that SGR increased at the mature green stage, and pART27-*SGR1* and pART27-*SGR2*-infiltrated fruit exhibited suppressed SGR protein activity. We observed that *CmSGR*-RNAi possessed residual green pigmentation in the epidermis at the breaker +7-day stage when compared to the WT. The *SGR* gene directly or indirectly affected a specific component of the CHL catabolic pathway and participated in a broad biological processes (Zhou et al., 2011). Expression of SGR increased at the mature green stage and reached its highest level at the Br stage, displayed ripening-induced expression. However, silencing the *CmSGR* gene using RNAi, delayed CHL breakdown during fruit ripening or leaf senescence; this result is consistent with that obtained using SGR1-RNAi in tomato fruits (Luo et al., 2013). We also performed quantitative PCR analysis to examine expression profiles. These results are consistent with previous observations in the literature. We found *SGR* to be expressed ubiquitously with melon fruit ripening. *CmSGR1* and *CmSGR2* were upregulated and promoted fruit ripening, and were not strongly expressed in the root and stem. Compared with other organs, *CmSGR3* and *CmSGR4* were expressed at lower levels during the course of melon fruit development, while *CmSGR3* and *CmSGR4* were more highly expressed in leaves, cotyledon, and stem than in fruit and root. *CmSGR* genes showed tissue-specific expression patterns in melon. Since the roots do not contain chloroplasts, there was minimal expression of the *CmSGR* genes in the roots. With fruit ripening, *CmSGR1* and *CmSGR2* play an important role in CHL degradation. *CmSGR3* and *CmSGR4* exhibit tissue-specific expression in leaves, cotyledon, and stem, but are not strongly expressed in fruit.

## Conflicts of interest

The authors declare no conflict of interest.

## ACKNOWLEDGMENTS

Research supported by the National Natural Science Foundation of China (#31560561).

## REFERENCES

- Akhtar MS, Goldschmidt EE, John I, Rodoni S, et al. (1999). Altered patterns of senescence and ripening in gf, a stay-green mutant of tomato (*Lycopersicon esculentum* Mill.). *J. Exp. Bot.* 50: 1115-1122. <http://dx.doi.org/10.1093/jxb/50.336.1115>
- Altschul SF, Gish W, Miller W, Myers EW, et al. (1990). Basic local alignment search tool. *J. Mol. Biol.* 215: 403-410. [http://dx.doi.org/10.1016/S0022-2836\(05\)80360-2](http://dx.doi.org/10.1016/S0022-2836(05)80360-2)
- Arabidopsis Genome Initiative (2000). Analysis of the genome sequence of the flowering plant *Arabidopsis thaliana*. *Nature* 408: 796-815. <http://dx.doi.org/10.1038/35048692>
- Arntzen CJ (1978). Dynamic structural features of chloroplast lamellae. *Curr. Top. Bioenerg.* 8: 112-155.
- Aubry S, Mani J and Hörtensteiner S (2008). Stay-green protein, defective in Mendel's green cotyledon mutant, acts independent and upstream of pheophorbide a oxygenase in the chlorophyll catabolic pathway. *Plant Mol. Biol.* 67: 243-256. <http://dx.doi.org/10.1007/s11103-008-9314-8>
- Bailey TL, Boden M, Buske FA, Frith M, et al. (2009). MEME SUITE: tools for motif discovery and searching. *Nucleic Acids Res.* 37: W202-8. <http://dx.doi.org/10.1093/nar/gkp335>
- Buchanan-Wollaston V (1997). The molecular biology of leaf senescence. *J. Exp. Bot.* 48: 181-199. <http://dx.doi.org/10.1093/jxb/48.2.181>
- Chenna R, Sugawara H, Koike T, Lopez R, et al. (2003). Multiple sequence alignment with the Clustal series of programs. *Nucleic Acids Res.* 31: 3497-3500. <http://dx.doi.org/10.1093/nar/gkg500>
- Finn RD, Bateman A, Clements J, Coggill P, et al. (2014). Pfam: the protein families database. *Nucleic Acids Res.* 42: D222-D230. <http://dx.doi.org/10.1093/nar/gkt1223>
- Garcia-Mas J, Benjak A, Sanseverino W, Bourgeois M, et al. (2012). The genome of melon (*Cucumis melo* L.). *Proc. Natl. Acad. Sci. USA* 109: 11872-11877. <http://dx.doi.org/10.1073/pnas.1205415109>
- Grassl J, Pružinská A, Hörtensteiner S, Taylor NL, et al. (2012). Early events in plastid protein degradation in stay-green *Arabidopsis* reveal differential regulation beyond the retention of LHCI and chlorophyll. *J. Proteome Res.* 11: 5443-5452. <http://dx.doi.org/10.1021/pr300691k>
- Hall TA (1999). BioEdit: a user-friendly biological sequence alignment editor and analysis program for Windows 95/98/NT. *Nucleic Acids Symp. Ser.* 41: 95-98.
- Hörtensteiner S (2009). Stay-green regulates chlorophyll and chlorophyll-binding protein degradation during senescence. *Trends Plant Sci.* 14: 155-162. <http://dx.doi.org/10.1016/j.tplants.2009.01.002>
- Hörtensteiner S and Kräutler B (2011). Chlorophyll breakdown in higher plants. *Biochim. Biophys. Acta* 1807: 977-988. <http://dx.doi.org/10.1016/j.bbapbio.2010.12.007>
- Hu L and Liu S (2011). Genome-wide identification and phylogenetic analysis of the ERF gene family in cucumbers. *Genet. Mol. Biol.* 34: 624-633. <http://dx.doi.org/10.1590/S1415-47572011005000054>
- Hu ZL, Deng L, Yan B, Pan Y, et al. (2011). Silencing of the LeSGR1 gene in tomato inhibits chlorophyll degradation and exhibits a stay-green phenotype. *Biol. Plant.* 55: 27-34. <http://dx.doi.org/10.1007/s10535-011-0004-z>
- Jiang H, Li M, Liang N, Yan H, et al. (2007). Molecular cloning and function analysis of the stay green gene in rice. *Plant J.* 52: 197-209. <http://dx.doi.org/10.1111/j.1365-3113X.2007.03221.x>
- Kusaba M, Ito H, Morita R, Iida S, et al. (2007). Rice NON-YELLOW COLORING1 is involved in light-harvesting complex II and grana degradation during leaf senescence. *Plant Cell* 19: 1362-1375. <http://dx.doi.org/10.1105/tpc.106.042911>
- Letunic I, Copley RR, Schmidt S, Ciccarelli FD, et al. (2004). SMART 4.0: towards genomic data integration. *Nucleic Acids Res.* 32: D142-D144. <http://dx.doi.org/10.1093/nar/gkh088>
- Lim PO, Woo HR and Nam HG (2003). Molecular genetics of leaf senescence in *Arabidopsis*. *Trends Plant Sci.* 8: 272-278. [http://dx.doi.org/10.1016/S1360-1385\(03\)00103-1](http://dx.doi.org/10.1016/S1360-1385(03)00103-1)

- Lim PO, Kim HJ and Nam HG (2007). Leaf senescence. *Annu. Rev. Plant Biol.* 58: 115-136. <http://dx.doi.org/10.1146/annurev.arplant.57.032905.105316>
- Luo Z, Zhang J, Li J, Yang C, et al. (2013). A STAY-GREEN protein SISGR1 regulates lycopene and b-carotene accumulation by interacting directly with SIPSY1 during ripening processes in tomato. *New Phytol.* 198: 442-452. <http://dx.doi.org/10.1111/nph.12175>
- Markwell JP, Thornber JP and Boggs RT (1979). Higher plant chloroplasts: Evidence that all the chlorophyll exists as chlorophyll-protein complexes. *Proc. Natl. Acad. Sci. USA* 76: 1233-1235. <http://dx.doi.org/10.1073/pnas.76.3.1233>
- Matile P (2000). Biochemistry of Indian summer: physiology of autumnal leaf coloration. *Exp. Gerontol.* 35: 145-158. [http://dx.doi.org/10.1016/S0531-5565\(00\)00081-4](http://dx.doi.org/10.1016/S0531-5565(00)00081-4)
- Park SY, Yu JW, Park JS, Li J, et al. (2007). The senescence-induced staygreen protein regulates chlorophyll degradation. *Plant Cell* 19: 1649-1664. <http://dx.doi.org/10.1105/tpc.106.044891>
- Pilkington SM, Montefiori M, Jameson PE and Allan AC (2012). The control of chlorophyll levels in maturing kiwifruit. *Planta* 236: 1615-1628. <http://dx.doi.org/10.1007/s00425-012-1723-x>
- Procházková D and Wilhelmová N (2007). Leaf senescence and activities of the antioxidant enzymes. *Biol. Plant.* 51: 401-406. <http://dx.doi.org/10.1007/s10535-007-0088-7>
- Pruzinská A, Tanner G, Aubry S, Anders I, et al. (2005). Chlorophyll breakdown in senescent *Arabidopsis* leaves. Characterization of chlorophyll catabolites and of chlorophyll catabolic enzymes involved in the degreening reaction. *Plant Physiol.* 139: 52-63. <http://dx.doi.org/10.1104/pp.105.065870>
- Ren G, An K, Liao Y, Zhou X, et al. (2007). Identification of a novel chloroplast protein AtNYE1 regulating chlorophyll degradation during leaf senescence in *Arabidopsis*. *Plant Physiol.* 144: 1429-1441. <http://dx.doi.org/10.1104/pp.107.100172>
- Rong H, Tang Y, Zhang H, Wu P, et al. (2013). The Stay-Green Rice like (SGRL) gene regulates chlorophyll degradation in rice. *J. Plant Physiol.* 170: 1367-1373. <http://dx.doi.org/10.1016/j.jplph.2013.05.016>
- Sakuraba Y, Schelbert S, Park SY, Han SH, et al. (2012). STAY-GREEN and chlorophyll catabolic enzymes interact at light-harvesting complex II for chlorophyll detoxification during leaf senescence in *Arabidopsis*. *Plant Cell* 24: 507-518. <http://dx.doi.org/10.1105/tpc.111.089474>
- Sato Y, Morita R, Nishimura M, Yamaguchi H, et al. (2007). Mendel's green cotyledon gene encodes a positive regulator of the chlorophyll-degrading pathway. *Proc. Natl. Acad. Sci. USA* 104: 14169-14174. <http://dx.doi.org/10.1073/pnas.0705521104>
- Saitou N and Nei M (1987). The neighbor-joining method: a new method for reconstructing phylogenetic trees. *Mol. Biol. Evol.* 4: 406-425.
- Schultz J, Milpetz F, Bork P and Ponting CP (1998). SMART, a simple modular architecture research tool: identification of signaling domains. *Proc. Natl. Acad. Sci. USA* 95: 5857-5864. <http://dx.doi.org/10.1073/pnas.95.11.5857>
- Sharma MK, Kumar R, Solanke AU, Sharma R, et al. (2010). Identification, phylogeny, and transcript profiling of ERF family genes during development and abiotic stress treatments in tomato. *Mol. Genet. Genomics* 284: 455-475. <http://dx.doi.org/10.1007/s00438-010-0580-1>
- Spano G, Di Fonzo N, Perrotta C, Platani C, et al. (2003). Physiological characterization of 'stay green' mutants in durum wheat. *J. Exp. Bot.* 54: 1415-1420. <http://dx.doi.org/10.1093/jxb/erg150>
- Tamura K, Stecher G, Peterson D, Filipski A, et al. (2013). MEGA6: Molecular Evolutionary Genetics Analysis version 6.0. *Mol. Biol. Evol.* 30: 2725-2729. <http://dx.doi.org/10.1093/molbev/mst197>
- Tang Y, Li M, Chen Y, Wu P, et al. (2011). Knockdown of OsPAO and OsRCCR1 cause different plant death phenotypes in rice. *J. Plant Physiol.* 168: 1952-1959. <http://dx.doi.org/10.1016/j.jplph.2011.05.026>
- Thomas H and Smart CM (1993). Crops that stay green. *Ann. Appl. Biol.* 123: 193-223. <http://dx.doi.org/10.1111/j.1744-7348.1993.tb04086.x>
- Zhou C, Han L, Pislariu C, Nakashima J, et al. (2011). From model to crop: functional analysis of a STAY-GREEN gene in the model legume *Medicago truncatula* and effective use of the gene for alfalfa improvement. *Plant Physiol.* 157: 1483-1496. <http://dx.doi.org/10.1104/pp.111.185140>

## Supplementary material

[Table S1](#). List of primers used in this study.

[Table S2](#). List of QPCR-primers used in this study.

[Table S3](#). List of protein sequences used in this study.